Available online at www.sciencedirect.com
ScienceDirect
Journal of the European Ceramic Society 29 (2009) 3121–3128
www.elsevier.com/locate/jeurceramsoc

Durability of clay roofing tiles: the influence of microstructural and compositional variables

M. Raimondo[a,*], C. Ceroni[b], M. Dondi[a], G. Guarini[a], M. Marsigli[c], I. Venturi[a], C. Zanelli[a]

[a] *CNR – Institute of Science and Technology for Ceramics, Via Granarolo, 64, 48018 Faenza, Italy*
[b] *Department of Applied Chemistry and Material Science, Engineering Faculty, University of Bologna, via Terracini, 28, 40138 Bologna, Italy*
[c] *CertiMaC, S.r.l., via Ravegnana, 186, 48018 Faenza, RA, Italy*

Received 5 February 2009; received in revised form 14 May 2009; accepted 10 June 2009

Abstract

The frost behaviour of 13 industrially manufactured roofing tiles was assessed through a double approach: performing severe freeze/thaw testing (EN 539-2) and calculating durability indices, according to models present in the literature. The products microstructure was fully investigated in terms of physical, technological and compositional parameters, and the results correlated with the frost resistance of roofing tiles. No prediction model was able to reliably foresee the product performances; in particular, the correspondence with the excellent experimental behaviour of the most resistant samples is lacking. Coupling microstructural with compositional variables, new indications came out concerning the design and production of roofing tiles able to withstand adverse climatic conditions. If, once again, bulk density can be considered as the most influent parameter (highest values involve an improved durability), the production of roofing tiles with excellent frost resistance involves also the evaluation of an increased number of product (i.e. raw materials composition, microstructure and phase composition) and processing (i.e. firing temperature) variables.

Keywords: Frost resistance; Traditional ceramics; Structural ceramics; Porosity; Microstructure-final

1. Introduction

Nowadays, clay roofing tiles are widely used as exterior building components and their durability, intended as the ability to withstand adverse climatic conditions, is one of the most important requirements to be considered in the structural design of modern buildings.[1,2] The deterioration of construction materials may be due to several factors; among them, design and construction techniques, environmental conditions and material properties may be, in most cases, considered predominant over other causes.[3] In particular, in cold climates, the service lifetime of clay-based components is heavily affected by frost action and salt crystallization.[4,5]

Frost action is produced when the temperature falls below 0 °C and the water included in the material porous structure starts freezing; the density change at the liquid–solid water transition implies the development of an internal pressure, leading to the formation of micro-cracks whose extent can overcome the mechanical resistance of the material, hence promoting inescapable damages.[6] The extent of these damages will be strictly dependent on the exposed surface area, as well as on the number and size of pores [7–9] and the saturation degree of the material.[9,10] For pore dimensions greater than a critical value and/or for a low saturation degree, the pressure developed, and hence damages, will be negligible since the free space within pores accommodates the expansion of the freezing water. On the opposite, when unfavourable climatic conditions are coupled with the presence of a high volume of capillary pores, the material ability to absorb water is increased[11] and severe structural damages, varying from surface scaling to complete disintegration, may occur. Owing to these circumstances, the material characteristics, which in turn depend on the raw material formulations,[12] the shaping process and the firing cycle,[13–15] become a key factor in the evaluation of the deterioration risk connected with frost action.[16–18]

Many papers in the field of civil engineering have analysed the factors affecting the durability of some construction materials (e.g. concrete), while freezing and thawing of

* Corresponding author. Tel.: +39 0546 699718; fax: +39 0546 46381.
E-mail address: mariarosa.raimondo@istec.cnr.it (M. Raimondo).

0955-2219/$ – see front matter © 2009 Elsevier Ltd. All rights reserved.
doi:10.1016/j.jeurceramsoc.2009.06.004

Table 1
Type and provenance of roofing tiles.

Sample	Product type	Clay origin
A	Marseilleuse	Switzerland
B	Portuguese	Veneto, Italy
C	Marseilleuse	Sicilia, Italy
D	Portuguese	Toscana, Italy
E	Portuguese	Basilicata, Italy
F	Marseilleuse	Lombardia/Emilia, Italy
G	Portuguese	Piemonte, Italy
H	Marseilleuse	Toscana, Italy
I	Portuguese	Toscana, Italy
J	Portuguese	Calabria, Italy
K	Coppo	Veneto, Italy
L	Marseilleuse	Marche, Italy
M	Portuguese	Portugal

other building components, such as roofing tiles, did not receive the same attention. Nevertheless, some authors – i.e. Maage,[19,20] Arnott,[21] Franke and Bentrup,[22,23] Koroth et al.,[24,25] Robinson,[26] Vincenzini[27] – have elaborated empirical prediction models which basically relate the frost resistance to technological (i.e. water absorption in different experimental conditions, capillary coefficient) or microstructural properties (i.e. porosity amount, size and internal specific surface of pores) of building materials. These models consist of equations able to quantify the product durability on the basis of calculated indices.

However, the results achieved and the choice of microstructural constraint ranges (e.g. median pore size, percentage of greater pores, etc.), expected to provide satisfactory performances, in most cases are not consistent with the material behaviour in the real working conditions; this implies the need of a deeper understanding of the material's structural and compositional properties, trying to overcome the limitation of using porosimetric investigations – if necessary coupled with technological tests – as main tool to predict frost performances. For these reasons, experimental investigations were performed combining the knowledge of both climate- and material-relevant parameters, with the objective to characterize the potential risk of frost decay.

This work is aimed at: (i) appraising the reliability of some prediction models available in the literature to foresee the frost resistance of industrially manufactured roofing tiles; (ii) comparing the results with the materials frost behaviour experimentally determined by severe freeze/thaw testing in climatic chamber; (iii) assessing the influence of material characteristics, in terms of pore amount, size and distribution, on their ability to withstand the frost action; (iv) evaluating the influence of compositional parameters – i.e. nature and relative amount of mineralogical phases – which in turn are linked to both product and processing conditions; (v) trying to give useful indications in the design of frost resistant clay-based components.

2. Materials and methods

13 industrially manufactured roofing tiles, coming from different manufacturing plants, were selected (Table 1). According with the different shape and colour, they have been classified as *Marseilleuse* (samples A, C, F, H and L), *Portuguese* (samples B, D, E, G, I, J and M) and *Coppo* (sample K) tiles. They were obtained by extrusion (*Coppo*) or by extrusion followed by a moulding step to get the final shape, and fired at a maximum temperature between 900 and 1050 °C, with a thermal cycle of 24–48 h from cold-to-cold.

Phase composition, open and total porosity, bulk density, pore size distribution and pore specific surface were determined on roofing tiles.

The phase composition was determined by X-ray powder diffraction (Rigaku DIII) under the following experimental conditions: monochromated Cu–$K_{1,2\alpha}$ radiation in the 5–80° 2θ range, scan rate 0.02° s^{-1}, 2 s per step. The quantitative analysis was performed by the RIR-Rietveld method adding 10 wt% of corundum (NIST 674) and using the GSAS software [28]; the experimental error is within 5% relative.

Open porosity (OP) and bulk density (BD) were quantified by measuring dry weight, water-saturated weight and the weight suspended in water, according to ASTM C373.[29] Specific weight (SW) was measured by He pycnometry (Micromeritics MVP 1305) according to ASTM C329[30] and total porosity (TP) was calculated by the equation: $TP = (1 - BD/SW) \times 100$.

The following porosity-related properties were measured: 24-h cold water absorption ($WA_{24\,h}$) and 5-h boiling water absorption ($WA_{5\,h}$) according to ASTM C67[31]; the ratio $WA_{24\,h}/WA_{5\,h}$ being defined as the saturation coefficient C_s. In addition, the 4-h cold water absorption (WA_{4h}) was determined.

The pore size distribution (in the 0.01–100 μm range) was determined by mercury intrusion porosimetry (ThermoFinningan Pascal 140 and 240) with an experimental uncertainty of about 1% relative; the experimentally measured mercury-brick contact angle of 166.4° was inserted into the Washburn equation.[32] Data were expressed as MD (medium pore diameter, μm), PV (cumulative volume of pores, cm^3/g), P3 (relative amount of pores having a diameter larger than 3 μm, %), Φ_{50} (median pore size, μm) and Φ_{90} (ninetieth percentile as calculated from the porosimetric distribution, μm); the pore specific surface (PSS) analysis was performed by nitrogen absorption (Micromeritics FlowSorb II 2300) following the B.E.T. single point method according to ASTM C1069.[33]

Capillary absorption was determined according to UNI 10859[34] on pieces of about 5 cm^3, obtained from each roofing tile. Samples were preventively dried in an electric oven at 60 ± 2 °C for 7 days and, after cooling, their weight was measured (m_0). A basal face of each one was put into direct contact with a 1 cm layer of paper, filled with distilled water at 20 °C, in a closed vessel in order to reach saturation conditions. The specimen's mass (m_i) was recorded after 10, 20, 30 and 60 min and plotted versus the square root of the elapsed time; the graph obtained presents an initial straight line, whose slope is the experimental capillary coefficient K_s.

Frost resistance was assessed by severe freeze/thaw testing, according to EN 539-2,[35] on 10 samples for each industrially manufactured roofing tile. Tests were carried out in a climatic cell at temperatures ranging from −15 to +15 °C performing 400 different freeze/thaw cycles; this number of cycles – much

Table 2
Prediction models and classification of frost behaviour as proposed by the authors.

Durability factor (DF)	Model: DF=	Frost resistant products	Frost susceptible products
Maage[19,20]	$3.2/PV + 2.4P3$	DF > 70	DF < 70
Arnott[21]	$9.2P3 - 0.5K_s + 423(WA_{5\,h}/WA) - 100K_sC_s - 84.5$	High values of DF	–
Franke and Bentrup[22,23]	Φ_{50} (porosimetric curve)	$\Phi_{50} \geq 1.65$ µm	$\Phi_{50} \leq 0.60$ µm
Koroth et al.[24,25]	$450(2.94 + WA_{5\,h}) + 330(1 - WA_{4\,h}/WA_{5\,h})$	DF > 85	DF < 70
Robinson[26]	$[K_s/10(1 - C_s)] + (WA_{24\,h} - 10)$	Low values of DF	–
Vincenzini[27]	Φ_{90} (porosimetric curve)	$\Phi_{90} \geq 1.80$ µm	$\Phi_{90} \leq 0.50$ µm

where PV (cm^3/g) = cumulative volume of pores; P3 (%) = relative amount of pores larger than 3 µm; K_s (g/cm^2 s$^{1/2}$) = capillary coefficient; $WA_{5\,h}$ (%) = 5-h boiling water absorption; WA (%) = water absorption; C_s (adim.) = saturation coefficient; Φ_{50} (µm) = median pore size; $WA_{4\,h}$ (%) = 4-h cold water absorption; $WA_{24\,h}$ (%) = 24-h cold water absorption; Φ_{90} (µm) = ninetieth percentile of porosimetric distribution.

Table 3
Open (OP) and total (TP) porosity, bulk density (BD), water absorption (WA), 24-h cold ($WA_{24\,h}$) and 5-h boiling water absorption ($WA_{5\,h}$), saturation coefficient (C_s) of roofing tiles.

Sample	OP (%)	TP (%)	BD (g/cm^3)	WA (%)	$WA_{24\,h}$ (%)	$WA_{5\,h}$ (%)	C_s (adim.)
A	20.3 ± 1.7	30.4 ± 0.4	1.877 ± 0.029	10.8 ± 1.1	10.7 ± 1.0	15.4 ± 0.1	0.69 ± 0.01
B	18.0 ± 0.2	25.1 ± 0.1	2.020 ± 0.002	8.9 ± 0.1	8.8 ± 0.1	11.1 ± 0.1	0.79 ± 0.01
C	27.8 ± 0.2	32.6 ± 0.2	1.817 ± 0.002	15.3 ± 0.1	14.9 ± 0.4	16.1 ± 0.2	0.92 ± 0.01
D	21.0 ± 0.4	29.6 ± 0.3	1.899 ± 0.015	11.1 ± 0.1	10.6 ± 0.1	11.4 ± 0.2	0.93 ± 0.01
E	13.0 ± 1.3	29.2 ± 0.2	1.910 ± 0.006	6.8 ± 0.7	8.0 ± 0.4	13.6 ± 0.4	0.59 ± 0.01
F	22.3 ± 0.8	29.1 ± 0.2	1.912 ± 0.010	11.7 ± 0.5	11.1 ± 0.2	13.0 ± 0.2	0.85 ± 0.01
G	19.3 ± 0.3	25.9 ± 0.2	1.997 ± 0.004	9.6 ± 0.2	10.1 ± 0.1	12.3 ± 0.2	0.82 ± 0.01
H	23.2 ± 0.5	29.6 ± 0.2	1.899 ± 0.004	12.2 ± 0.2	12.2 ± 0.5	14.3 ± 0.3	0.85 ± 0.01
I	21.1 ± 0.7	27.2 ± 0.1	1.962 ± 0.001	10.8 ± 0.4	11.1 ± 0.4	13.1 ± 0.1	0.85 ± 0.01
J	25.2 ± 0.6	31.0 ± 0.2	1.861 ± 0.003	13.5 ± 0.3	13.1 ± 0.6	14.7 ± 0.1	0.89 ± 0.01
K	24.3 ± 0.8	29.7 ± 0.2	1.895 ± 0.007	12.8 ± 0.4	11.6 ± 0.6	14.5 ± 0.6	0.80 ± 0.01
L	22.4 ± 0.3	28.6 ± 0.2	1.924 ± 0.010	11.7 ± 0.2	11.6 ± 0.2	13.5 ± 0.2	0.86 ± 0.01
M	19.4 ± 0.5	23.2 ± 0.2	2.070 ± 0.008	9.3 ± 0.3	9.9 ± 0.2	11.1 ± 0.2	0.89 ± 0.01

higher than those (150) scheduled by the reference standard EN 539-2 – was chosen in order to simulate extreme conditions. The frost resistance was expressed as the number of overcome freezing/thaw cycles, followed by the analysis of both the mass loss and the structural changes or damages standing out during and after the test.

Both microstructural and porosity-related parameters were utilized to calculate durability indices according to the models proposed by Maage,[19,20] Arnott,[21] Franke and Bentrup,[22,23] Koroth et al.,[24,25] Robinson,[26] and Vincenzini.[27] The variables considered by the authors to elaborate their models and to calculate durability factors are summarized in Table 2.

A statistical elaboration of data was performed by simple (linear binary correlation) and multivariate analysis techniques (factor and multiple regression analyses) using the StatSoft Statistica 6.0 software. Factor analysis was carried out on the main physical, compositional and microstructural variables extracting principal components (three factors according to the screen test for eigenvalues). Multiple linear regression was executed by the

Table 4
Medium pore diameter (MD), cumulative volume of pores (PV), relative amount of pores having a diameter larger than 3 µm (P3), Φ_{50} (median pore size), Φ_{90} (ninetieth percentile of the porosimetric distribution), pore specific surface (PSS) and capillary coefficient (K_s) of roofing tiles.

Sample	MD (µm)	PV (cm^3/g)	P3 (%)	Φ_{50} (µm)	Φ_{90} (µm)	PSS (m^2/g)	K_s (g/cm^2 s$^{1/2}$)
A	1.9	0.146	56.0	1.8	4.5	0.7	5.8
B	0.5	0.134	3.3	0.5	1.2	1.7	2.2
C	0.4	0.189	0.7	0.4	0.8	1.8	5.2
D	0.3	0.161	1.6	0.4	0.7	1.6	2.6
E	0.7	0.151	14.2	0.5	3.0	1.1	0.1
F	0.4	0.157	2.4	0.4	0.8	1.5	4.5
G	0.7	0.132	12.9	0.7	3.5	1.6	0.8
H	0.5	0.168	1.9	0.5	1.3	1.2	4.0
I	0.4	0.146	2.4	0.4	1.2	1.8	4.8
J	0.4	0.182	3.1	0.4	0.8	1.6	4.4
K	0.4	0.179	1.4	0.4	0.7	1.3	3.0
L	0.4	0.161	2.4	0.4	0.9	1.8	3.6
M	0.3	0.117	8.6	0.3	1.4	2.2	3.3

Table 5
Phase composition of roofing tiles (wt%).

Sample	Quartz	K-feldspar	Plagioclase	Pyroxene	Hematite	Illite/Mica	Gehlenite	Amorphous
A	38	8	22	14	4	–	–	14
B	24	3	11	1	5	13	–	42
C	26	7	33	12	2	5	6	8
D	20	5	22	32	5	–	1	17
E	33	7	30	3	2	–	1	23
F	24	7	26	3	3	–	–	37
G	42	13	5	6	7	–	–	27
H	23	6	41	2	2	–	2	24
I	31	6	19	1	6	9	–	27
J	20	6	36	1	1	8	–	27
K	6	1	24	9	2	–	–	58
L	24	4	44	2	2	–	1	23
M	39	7	–	–	4	10	–	40

forward stepwise method, including intercept in the model and setting $F = 1$ to enter.[36]

3. Results and discussion

3.1. Physical properties and phase composition of roofing tiles

Physical and porosimetric properties of roofing tiles are summarized in Tables 3 and 4, respectively. Total porosity is in the 23–33% range, mostly represented by open porosity (13–28%); water absorption follows the same trend of open porosity, while the saturation coefficient C_s varies in the 0.7–0.9 range.

A more detailed analysis of pore dimensions highlights the relative differences in terms of both medium pore size (from 0.3 μm of samples D, M to 1.9 μm of sample A) and percentage of big pores (from 0.7% of sample C to 56% of sample A), also involving a different pore morphology as expressed by the values of PSS (0.7–2.2 m^2/g).

Phase composition of roofing tiles shows a wide variability of the amounts of both new formed and residual components (Table 5). Samples are made up of residual quartz (6–42%), K-feldspar (up to 13%) and, in some samples, illite/mica (sample B has a content as high as 13%). The amount of the amorphous phase ranges from 8% (sample C) to 58% (sample K). New formed crystalline phases are: plagioclase (Ca-rich terms close to anorthite[39] up to 44%), clinopyroxene (‘fassaitic’ terms[40] up to 32%) and melilite (a gehlenite–akermanite solid solution[41] up to 6%); the total amount of Ca-silicates, i.e. the sum plagioclase + pyroxene + gehlenite, goes from 0% (sample M) to 55% (sample D).

3.2. Frost resistance of roofing tiles

Looking at the frost resistance of roofing tiles in terms of number of passed cycles with respect to the total number of freeze/thaw cycles (Table 6), different performance levels are outlined: (i) samples A, D and H have excellent performances since they were able to overcome 400 freeze/thaw cycles with no or few defects; (ii) sample B shows a similar behaviour, being able to overcome 375 cycles; (iii) a still good resistance was shown by samples E and L (275 cycles), while F, G, J, K were able to pass no more than 100 cycles; (iv) the lowest frost resistance belongs to samples I (75 cycles), M (50 cycles) and C (25 cycles).

Table 6
Frost resistance of roofing tiles determined according to EN 539-2.

Sample	Number of freeze/thaw cycles	Passed freeze/thaw cycles	Defects found after freeze/thaw testing[a]
A	400	400	Several chips on the back of the sample
B	400	375	Loss of interlocking ribs, hair cracks
C	50	25	Big exfoliations on both sample sides
D	400	400	None
E	300	275	Several exfoliations on both sample faces
F	125	100	Loss of interlocking ribs, delaminations, flaking, hair cracks
G	125	100	Breaking of test sample into three pieces
H	400	400	Detachment of a sample projection
I	100	75	Exfoliations, hair cracks
J	125	100	Delaminations, exfoliations, hair cracks, loss of interlocking ribs
K	125	100	Surface cracks, delaminations, exfoliations, structural cracks, pits
L	300	275	Exfoliations, loss of interlocking ribs, hair cracks
M	150	50	Loss of interlocking ribs, chips, hair cracks, delaminations

[a] The weight loss after freeze/thaw cycles was below 1% for all samples.

Table 7
Durability indices of roofing tiles.

Sample	Durability factors					
	Maage	Arnott	Franke–Bentrup	Koroth et al.	Robinson	Vincenzini
A	156	962	1.8	220	0.9	4.5
B	32	394	0.5	288	−1.2	1.2
C	19	273	0.4	238	4.9	0.8
D	24	272	0.4	277	0.6	0.7
E	55	835	0.5	355	−2.0	3.0
F	26	321	0.4	233	1.1	0.8
G	55	495	0.7	328	0.1	3.5
H	24	343	0.5	254	2.0	1.3
I	28	365	0.4	227	1.2	1.2
J	25	314	0.4	246	1.7	0.8
K	21	327	0.4	279	3.1	0.7
L	26	339	0.4	259	1.7	0.9
M	48	410	0.3	255	−0.1	1.4

3.3. Reliability of prediction models

In order to assess both reliability and validity range of the models (Table 2), a comparison between the experimental results – in terms of number of freeze/thaw cycles passed – and the calculated indices (Table 7) was undertaken. Looking at Fig. 1, the following considerations can be drawn out:

Maage's durability factor, although presents a positive relationship with the number of freeze/thaw cycles, is not able to discriminate among frost (DF > 70) and non-frost resistant (DF < 70) products,[37,38] with sample A being the only one that can be considered as frost resistant. The model provides no reasons of the excellent performances (400 cycles) of the samples B, D and H. Looking in detail at the microstructure of sample A (Table 4), it is clear that Maage's factor mainly accounts for its very high percentage of pores having a diameter greater than 3 μm (P3 = 56%).

No significant trend was detected plotting the durability factor, calculated according to Robinson's model, versus the experimental behaviour of samples; as supposed by the author, the index seems to decrease when the behaviour of products improves. Theoretically, the negative trend predicted by the model depends on both the K_s and WA parameters, which are expected to be as low as possible for highly resistant porous structures. The rate of the water suction, expressed by K_s, and the water absorption capacity are connected with the presence, respectively, of capillary and open pores, which are deleterious for the products performances in adverse environmental conditions.

The model proposed by Arnott – obtained through a multiple regression analysis of different physical and technological parameters with the role of each variable being quantified by a statistical different weight – seems to present a good agreement with the experimental performances of poor resistant (≤100 cycles, samples C, F, M, G, I, J, K) and some highly resistant (>250 cycles, samples A and E) products. However, it results not suitable to explain the excellent performances of samples L, B, H and D.

Table 8
Extraction of the main components: factorial weights.

Variable	Factorial weights		
	Factor 1	Factor 2	Factor 3
Freeze/thaw cycles	0.535	−0.001	0.457
TP	0.545	−0.794	−0.123
P3	0.813	0.495	0.056
PSS	−0.837	0.040	−0.438
BD	−0.542	0.794	0.127
Φ_{50}	0.864	0.381	0.115
Quartz	0.250	0.793	−0.528
Ca-silicates	0.457	−0.841	−0.008
Amorphous	−0.610	0.178	0.691
Φ_{90}	0.707	0.649	−0.042
Variance	4.132	3.446	1.214

The models considering the porosimetric parameters Φ_{50}[22] and Φ_{90}[27] as the main criteria to discriminate among frost and non-frost resistant products revealed to be not reliable: the correspondence between the experimental performances and the limits proposed by Vincenzini ($\Phi_{90} \geq 1.8$ μm for frost resistant and $\Phi_{90} \leq 0.5$ μm for non-frost resistant products) can be validated just for samples A and E, while sample G, although presenting a Φ_{90} value as high as 3.5 μm, does not show a good real durability. Analogously, the trend shown by median pore size values Φ_{50} presents, more or less, the same limitations of Maage's factor; in fact, A is the only sample which can be considered as frost resistant ($\Phi_{50} \geq 1.65$ μm), while the behaviour of G needs deeper investigations. The experimental results indicate that good (samples E and L) or excellent (samples B, D, H) performances belong to products having a reduced value of pore size ($\Phi_{50} \leq 0.5$–0.6 μm).

Finally, according to Koroth's et al. model,[24,25] all samples should be considered as frost resistant, since the durability factor calculated for each of them is much higher than the limit value of 85; however, this circumstance does not correspond to the experimental performances of samples.

3.4. Statistical treatment of physical and technological variables

Since simple binary correlations between the calculated indices and the experimental behaviour of roofing tiles were not satisfactory, a statistical elaboration of data (factor and "stepwise" multiple regression analyses) was undertaken considering, besides the number of freeze/thaw cycles, physical (TP, BD, P3, BET, Φ_{50} and Φ_{90}) and compositional (amount of quartz, amorphous phase and Ca-silicates) properties of products as well.

The extraction of the principal components (Table 8) highlights that, as expected, the frost resistance of products is correlated in a quite complex way with many variables so that the hypothesis that more than one parameter could simultaneously influence the materials real performances is in some way confirmed.

Anyway, looking at the mutual relationships between factors 1 and 2 (Fig. 2), the following conclusions can be drawn out:

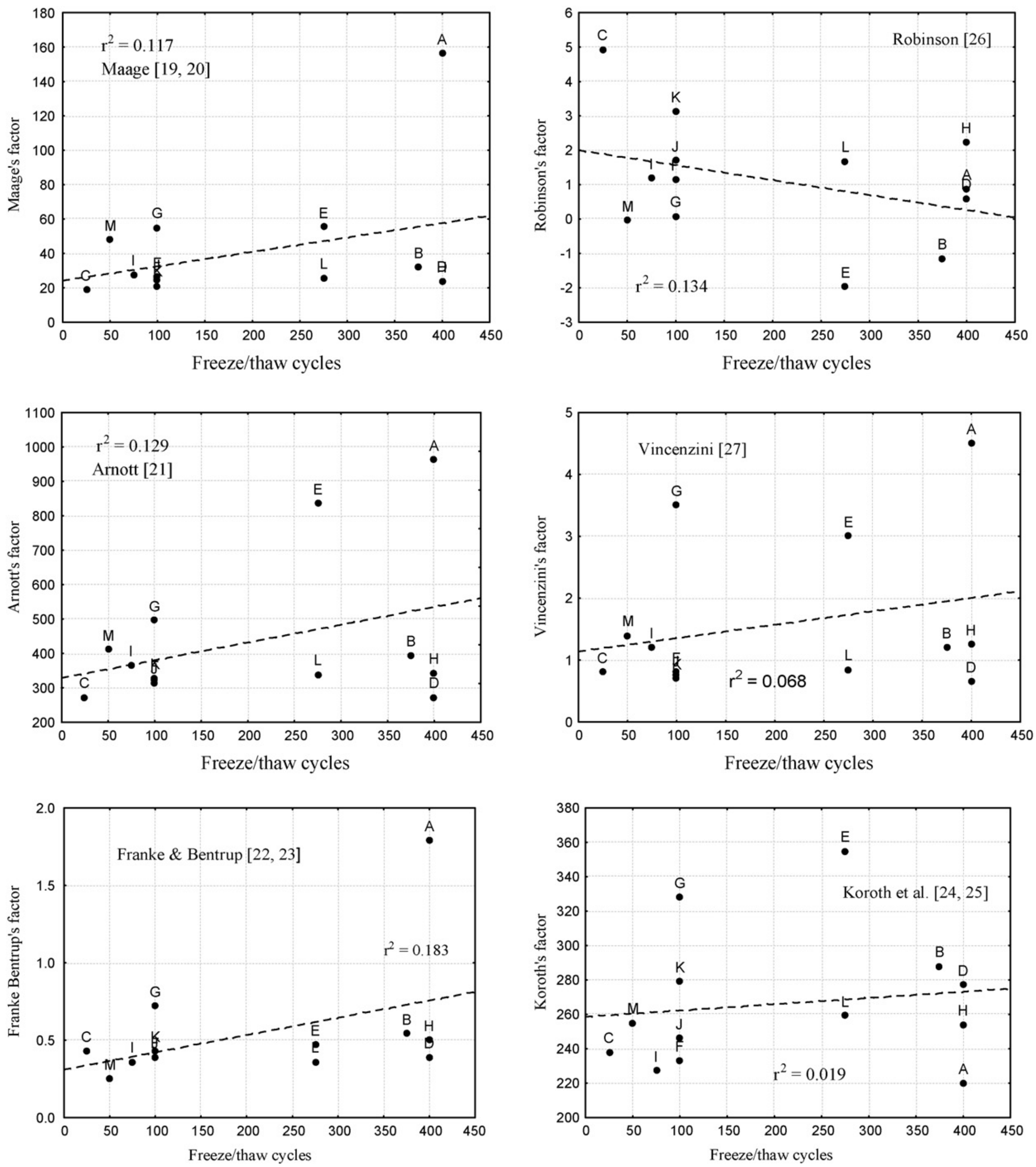

Fig. 1. Experimental behaviour of roofing tiles (number of freeze/thaw cycles passed) vs. durability factors.

- a positive correlation seems to exist between the number of freeze/thaw cycles and the amount of pores greater than 3 μm (P3), the median pore size (Φ_{50}) and Φ_{90} values;
- frost resistance is inversely related not only to the pore specific surface (PSS) but also to the amount of amorphous phase, so that the highest its content the lowest the product performances;
- the role played by quartz amount and Ca-silicates is more ambiguous so that in this stage these variables seem do not directly affect the frost resistance.

The results of the multiple regression analysis ($R^2 = 0.941$, $p < 0.002$), taking into account the product frost resistance as dependent variable and the physical and compositional parameters as independent ones, made possible to confirm some of these indications (Table 9):

- the statistical procedure selected the following as the most influent parameters: BD, PSS, Φ_{50} together with quartz, Ca-silicates and amorphous amounts;

Table 9
Results of the multiple regression analysis.

Stepwise multiple regression analysis; $R = 0.970$; $R^2 = 0.941$; p-level < 0.0020 ($N = 13$)					
$N = 13$	β	Std. error	B	Std. error	p-Level
Intercept			−7063.22	1052.63	0.0005
PSS	−0.821	0.201	−338.80	83.12	0.0065
Amorphous	−0.775	0.381	−9.20	4.53	0.0885
BD	1.857	0.231	4227.63	527.29	0.0002
Quartz	−0.882	0.368	−14.33	5.98	0.0054
Ca-silicates	0.779	0.223	7.34	3.99	0.0110
Φ_{50}	0.252	0.182	101.05	73.41	0.2180

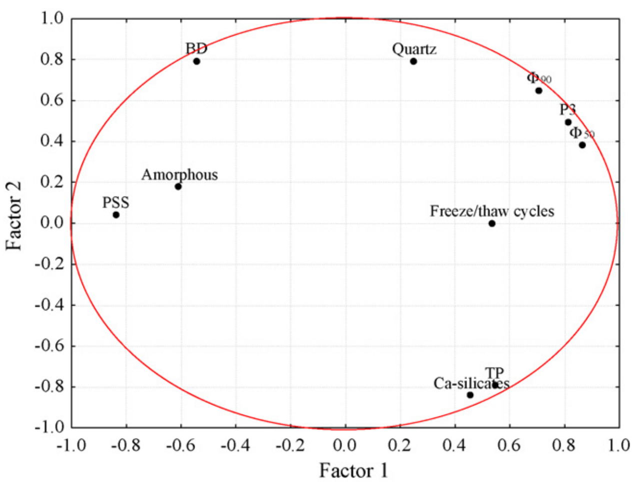

Fig. 2. Extraction of the main components: factor 1 vs. factor 2. The total variance explained by factors 1 and 2 is about 76%.

- among the selected variables and according to the β factors, BD results to be the most influent; however, the statistical weights of the mineralogical phases are not negligible since they are quantitatively equivalent to that of PSS and prevailing on that selected for pore size (Φ_{50});
- concerning the positive or negative role played by each selected variable, it is confirmed that the amount of Ca-silicates, on one side, and those of quartz and amorphous, on the other side, work in the opposite way; a higher amount of new formed phases increases the frost resistance of products, while the presence of both quartz and amorphous potentially involves the risk of frost damages;
- the evaluation of the p-level corresponding to each selected parameter (probably with the only exception of Φ_{50}), allows to assess the reliability of the statistical procedure in predicting the materials frost behaviour.

Following these results, it can be pointed out that the production of roofing tiles with excellent frost resistance – which are able to overcome a number of freeze/thaw cycles much higher that those required by the current standard – involves the evaluation of both product and processing variables. As far as the composition of raw mixtures, their CaO content should be optimized paying a great attention to the development of a highly porous microstructure and controlling the pore dimensions (to get lower PSS values). Analogously, the amount of new formed Ca-silicates should be promoted ($\geq$40%), while the amount of amorphous phase reduced under about 20%. These components play an important, although often neglected role in frost behaviour, that is usually concerned with porosity alone. It is the ceramic matrix to withstand mechanical stress due to ice crystallization and factors affecting its stability and mechanical properties should be considered too. It was observed that Ca-silicates improve the degree of sintering of ceramic necks around pores, so enhancing mechanical strength, and that Ca-rich bodies are stronger than Ca-poor ones for the same amount of porosity.[42,43] On the other hand, the amorphous phase is prone to rehydration processes and it is the main cause of long-term expansion of roof tiles, also affecting durability.[43] However, reducing the amorphous phase is not straightforward, since its amount varies with firing temperature, depending also on body composition. Ca-rich bodies usually exhibit low amounts of amorphous phase, which are minimum in a wide range of firing temperatures (900–1100 °C); in contrast, the amount of amorphous phase is generally greater in Ca-poor bodies and is rapidly increasing over 1000 °C, as liquid phase develops.[39,42]

The phase composition requirements, together with the need to obtain a microstructure having a higher quantity of pores greater than 3 μm, can be satisfied through the modification of the firing process, e.g. increasing the maximum firing temperature and, to a lesser extent, prolonging the soaking time.

4. Conclusions

The frost behaviour (EN 539-2) of 13 industrially manufactured roofing tiles was assessed and the experimental results contrasted with durability indices calculated according to literature models. No model is able to reliably predict the frost performances since they exhibit a strong dependence on the data population and probably succeed only with homogeneous samples in terms of both composition and manufacturing technology.

The limitation connected with the utilization of porosimetry or technological tests, as main tools to predict the frost resistance, can be by-passed only through a more extensive analysis of materials physical and compositional properties. This approach was pursued by a statistical procedure involving all the microstructural and compositional variables, together with the experimental number of freeze/thaw cycles, so that new indications came out concerning the design and production of roofing tiles able to withstand adverse climatic conditions. If bulk density has to be still considered as one of the most influent parameter, the role of phase composition, in terms of amounts of residual and new formed phases, turns to be determinant. This circumstance has it out with the influence of both product and processing variables on the development of the suitable microstructure to get the best durability against frost action: the CaO content of raw materials should be optimized for the development of a highly porous microstructure promoting in the same time the formation of Ca-silicates above 40%; the amount of amorphous phase should be reduced under about 20%. These requirements, together with the need to obtain a high quantity of pores greater than 3 μm, can be satisfied through the modification of the firing process, e.g. increasing the maximum firing temperature.

References

1. Quenard, D. A., Xu, K., Kiinzel, H. M., Bentz, D. P. and Martys, N. S., Microstructure and transport properties of porous building materials. *Mater. Struct./Mater. Construct.*, 1998, **31**, 317–324.
2. Lisø, K. R., Kvande, T., Hygen, H. O., Thue, J. V. and Harstveit, K. A., Frost decay exposure index for porous, mineral building materials. *Build. Environ.*, 2007, **42**, 3547–3555.
3. Elert, K., Cultrone, G., Rodriguez Navarro, C. and Pardo, E. S., Durability of bricks used in the conservation of historic buildings—influence of composition and microstructure. *J. Cultural Heritage*, 2003, **4**, 91–99.
4. LÜ, X. and Viljanen, M., Determination of salt diffusion coefficient in brick: analytical methods. *Transport Porous Media*, 2002, **49**, 241–246.
5. Larsen, E. S. and Nielsen, C. B., Decay of bricks due to salts. *Mater. Struct.*, 1990, **23**, 16–21.
6. Setzer, M. J., Micro-ice-lens formation in porous solid. *J. Colloid Interface Sci.*, 2001, **243**, 193–201.
7. Sveda, M., Influence of pore structure on the frost resistance of brick products. *Ziegelindustrie Int.*, 1999, **7**, 80–85.
8. Nakamura, M., Indirect evaluation of frost susceptibility of building materials. *Am. Ceram. Soc. Bull.*, 1988, **67**(12), 1664–1965.
9. Gummerson, R. J., Hall, C. and Hoff, W. D., The suction rate and the absorption of bricks. *Br. Ceram. Trans. J.*, 1981, **80**, 150–151.
10. Hoffman, D. and Niesel, K., Quantifying capillary rise in columns of porous material. *Am. Ceram. Soc. Bull.*, 1988, **67**(8), 1418.
11. Raimondo, M., Dondi, M., Gardini, D. and Guarini, G., Predicting the initial rate of water absorption. In A.N. Turkeri, and O. Segul (Eds.), Proceedings of 11DBMC International Conference on Durability of Building Materials and Components, Globality and locality in durability, CD-ROM, Istanbul, 2008.
12. Freyburg, S. and Schwarz, A., Influence of the clay type on the pore structure of structural ceramics. *J. Eur. Ceram. Soc.*, 2006, **27**, 1727–1733.
13. Beltrán, V., Barba, A., Jarque, J. C. and Escardino, A., Liquid suction by porous ceramic materials. 3. Influence of the nature of the composition and the preparation method of the pressing powder. *Br. Ceram. Trans. J.*, 1991, **90**, 77–80.
14. Beltrán, V., Barba, A., Rodrigo, M. D. and Escardino, A., Liquid suction by porous ceramic materials. 2. Influence of pressing conditions. *Br. Ceram. Trans. J.*, 1989, **88**, 219–222.
15. Escardino, A., Beltrán, V., Barba, A. and Sánchez, E., Liquid suction by porous ceramic materials. 4. Influence of firing conditions. *Br. Ceram. Trans. J.*, 1999, **98**(5), 225–229.
16. Ikeda, K., Kim, H. S. and Kaizu Higashi, K. A., Influence of firing temperature on frost resistance of roofing tiles. *J. Eur. Ceram. Soc.*, 2004, **24**, 3671–3677.
17. Cultrone, G., Sebastián, E., Elert, K., de la Torre, M. J., Cazalla, O. and Rodriguez-Navarro, C., Influence of mineralogy and firing temperature on the porosity of bricks. *J. Eur. Ceram. Soc.*, 2004, **24**, 547–564.
18. Tang, F., Fudouzi, H., Uchikoshi, T. and Sakka, Y., Preparation of porous materials with controlled pore size and porosity. *J. Eur. Ceram. Soc.*, 2004, **24**, 341–344.
19. Maage, M., Frost resistance and pore size distribution in bricks. Part 1. *Ziegelindustrie Int.*, 1990, **9**, 472–481.
20. Maage, M., Frost resistance and pore size distribution in bricks. Part 2. *Ziegelindustrie Int.*, 1990, **10**, 582–588.
21. Arnott, M., Investigation of freeze-thaw durability, In NRC-IRC Report N. CR 5680.1, Nat. Res. Council of Canada, Ottawa, Canada, 1990.
22. Franke, L. and Bentrup, H., Evaluation of the frost resistance of bricks in regard to long service life. Part 1. *Ziegelindustrie Int.*, 1993, **7–8**, 483–492.
23. Franke, L. and Bentrup, H., Evaluation of the frost resistance of bricks in regard to long service life. Part 2. *Ziegelindustrie Int.*, 1993, **9**, 528–536.
24. Koroth, R., Fazio, P. and Fedman, D., Development of new durability index for clay bricks. *J. Architect. Eng.*, 1988, **9**, 87–93.
25. Koroth, R., Fazio, P. and Fedman, D., Comparative study of durability indices of clay bricks. *J. Architect. Eng.*, 1998, **9**(1), 26–33.
26. Robinson, G. C., Relation between physical properties and durability of commercial marketed bricks. *Am. Ceram. Soc. Bull.*, 1995, **56**(12), 1071–1075.
27. Vincenzini, P., Le prove di laboratorio nella previsione del comportamento al gelo dei materiali ceramici per l'edilizia. *Ceramurgia*, 1974, **3**, 176–188.
28. Larson, A. C. and Von Dreele, R. B., General Structure Analysis System (GSAS). Los Alamos National Laboratory Report, LAUR 2000, pp. 86–748.
29. ASTM C373, *Water Absorption, bulk density, apparent porosity and apparent specific gravity of fired whiteware products*. American society for Testing and Materials, 1994.
30. ASTM C329, *Specific gravity of fired ceramic whiteware materials*. American Society for Testing and Materials, 1994.
31. ASTM C67, *Standard test methods for sampling and testing bricks and structural clays*. American Society for Testing and Materials, 1996.
32. Washburn, E. W., Note on a method of determining the distribution of pore sizes in a porous material. *Proc. Natl. Acad. Sci. USA*, 1921, **7**, 115–116.
33. ASTM C 1069, *Specific surface area of alumina or quartz by nitrogen adsorption*. American Society for Testing and Materials, 1997.
34. UNI 10859, *Cultural heritage – Natural and Artificial Stones – Determination of Water Absorption by Capillarity*. UNI Ente Italiano di Unificazione, 2000.
35. UNI EN 539-2, Clay roofing tiles for discontinuous laying. *Determination of Physical Characteristics. Part 2. Test for Frost Resistance*. UNI Ente Italiano di Unificazione, 2000.
36. Cooley, W. W. and Lohnes, P. R., *Multivariate data analysis*. John Wiley and Sons, New York, 1971.
37. Winslow, D. N., Kilgour, C. L. and Crooks, R. W., Predicting the durability of bricks. *J. Test. Eval.*, 1988, **16**(6), 527–531.
38. Winslow, D. N., Predicting the durability of paving bricks. *J. Test. Eval.*, 1991, **19**(1), 29–33.
39. Dondi, M., Guarini, G. and Raimondo, M., Trends in the formation of crystalline and amorphous phases during the firing of clay bricks. *Tile Brick Int.*, 1999, **15**(3), 176–183.
40. Dondi, M., Ercolani, G., Fabbri, B. and Marsigli, M., An approach to the chemistry of pyroxenes formed during the firing of Ca-rich silicate ceramics. *Clay Miner.*, 1998, **33**, 443–452.
41. Dondi, M., Ercolani, G., Fabbri, B. and Marsigli, M., Chemical composition of melilite formed during the firing of carbonate-rich and iron-containing ceramic bodies. *J. Am. Ceram. Soc.*, 1999, **82**(29), 465–468.
42. Dondi, M., Marsigli, M. and Venturi, I., Firing behaviour of Italian clays used in brick and roofing tile production. *L'Industria dei Laterizi*, 1998, **54**, 382–394.
43. Dondi, M., Ercolani, G., Guarini, G., Marsigli, M. and Venturi, I., Microstructural evolution during fast firing of porous tile bodies. *Ceramurgia*, 1995, **25**(6), 301–314 [in Italian].